Cyclic strain induces dual-mode endothelial-mesenchymal transformation of the cardiac valve

Kartik Balachandran[a], Patrick W. Alford[a], Jill Wylie-Sears[b,c], Josue A. Goss[a], Anna Grosberg[a], Joyce Bischoff[b,c], Elena Aikawa[c,d], Robert A. Levine[c,e], and Kevin Kit Parker[a,1]

[a]Disease Biophysics Group, Wyss Institute for Biologically Inspired Engineering, School of Engineering and Applied Sciences, Harvard University, Cambridge, MA 02138; [b]Vascular Biology Program and Department of Surgery, Children's Hospital Boston, Boston, MA 02115; [c]Harvard Medical School, Boston, MA 02115; [d]Cardiovascular Medicine, Brigham and Women's Hospital, Boston, MA 02115; and [e]Cardiac Ultrasound Laboratory, Massachusetts General Hospital, Boston, MA 02114

Edited by Robert Langer, Massachusetts Institute of Technology, Cambridge, MA, and approved October 3, 2011 (received for review June 9, 2011)

Endothelial-mesenchymal transformation (EMT) is a critical event for the embryonic morphogenesis of cardiac valves. Inducers of EMT during valvulogenesis include VEGF, TGF-β1, and wnt/β-catenin (where wnt refers to the wingless-type mammary tumor virus integration site family of proteins), that are regulated in a spatiotemporal manner. EMT has also been observed in diseased, strain-overloaded valve leaflets, suggesting a regulatory role for mechanical strain. Although the preponderance of studies have focused on the role of soluble mitogens, we asked if the valve tissue microenvironment contributed to EMT. To recapitulate these microenvironments in a controlled, in vitro environment, we engineered 2D valve endothelium from sheep valve endothelial cells, using microcontact printing to mimic the regions of isotropy and anisotropy of the leaflet, and applied cyclic mechanical strain in an attempt to induce EMT. We measured EMT in response to both low (10%) and high strain (20%), where low-strain EMT occurred via increased TGF-β1 signaling and high strain via increased wnt/β-catenin signaling, suggesting dual strain-dependent routes to distinguish EMT in healthy versus diseased valve tissue. The effect was also directionally dependent, where cyclic strain applied orthogonal to axis of the engineered valve endothelium alignment resulted in severe disruption of cell microarchitecture and greater EMT. Once transformed, these tissues exhibited increased contractility in the presence of endothelin-1 and larger basal mechanical tone in a unique assay developed to measure the contractile tone of the engineered valve tissues. This finding is important, because it implies that the functional properties of the valve are sensitive to EMT. Our results suggest that cyclic mechanical strain regulates EMT in a strain magnitude and directionally dependent manner.

tight junctions | cytokines | activated myofibroblast

Cardiac valves are sophisticated structures that function in a complex mechanical environment, opening and closing more than 3 billion times during the average human lifetime (1). Initially considered passive flaps of tissue, it is now acknowledged that valves contain a highly heterogeneous population of endothelial (VEC) and interstitial (VIC) cells. The VICs exist as synthetic, myofibroblast, or smooth muscle-like phenotypes (2, 3) and alter their tone in response to vasoactive mediators (4–7). The VECs line the surface of the valve leaflet and are unique in their ability to undergo endothelial-mesenchymal transformation (EMT), a process that is crucial for valvulogenesis (8, 9). Recent clinical evidence of EMT has been observed in pathologies such as ischemic cardiomyopathy and concomitant mitral regurgitation and is correlated with increased leaflet mechanical strains (10, 11). These pathological strains can be oriented obliquely to cell and tissue orientation (12, 13), suggesting the possible interaction between mechanical forces and tissue architecture in regulating EMT.

Prior work has focused on the regulation of EMT via soluble factors. Modulation of VEGF and increases in wnt/β-catenin and TGF-β1 expression, among other factors, direct EMT during valvulogenesis (8, 14) and in the mature valve (15, 16). Additionally, mechanical forces are known to modulate valve remodeling and disease progression (17, 18). However, the influence of mechanical forces and its synergy with tissue architecture in influencing cardiac valve EMT is unknown. During embryonic development, valve morphogenesis has been correlated with an increase in fluid shear stresses, mechanical strains, and altered geometry of the developing heart (19–22). These observations potentially suggests interaction between mechanical forces and the factors that regulate EMT. Additionally, it is also unknown if EMT results in a functional change of the VEC to a contractile myofibroblast-like VIC.

We hypothesized that cyclic strain may potentiate valve EMT in a manner dependent on cell orientation and the direction of applied strain. We developed an in vitro model that combines cyclic stretching of engineered valve endothelium reconstituted from primary sheep VECs for biochemical and expression studies. In addition, we present a functional assay for EMT using valve thin films (vTFs), a biohybrid construct of the engineered valve endothelium on an elastomer thin film that is deformed during tissue contraction. We report strain-dependent dual-mode EMT, with TGF-β1 signaling triggering EMT under low strain (10%) and wnt/β-catenin signaling under high strain (20%). We also report strain-dependent increased contractility of transformed VEC tissues when treated with endothelin-1, suggesting transformation of the normally noncontractile VEC to a contractile VIC-like cell.

Results

In Vitro Model for Engineered Valve Endothelium. VECs typically align perpendicular to flow (23, 24), resulting in an anisotropic alignment on the inflow surface that is oriented circumferential to the valve leaflet (23, 25). VECs in the outflow surface generally exhibit no preferred orientation and are isotropic (23) due to oscillatory blood flow patterns (26). Mechanical stresses are oriented circumferentially in the healthy valve and are altered from increased hemodynamic pressures or aberrant deformations due to altered wall stresses during the contractile cycle during ischemic cardiomyopathy. These altered stresses typically manifest as altered strains (1, 12, 13, 27). In an attempt to mimic this cell microenvironment in a simplified model, we engineered 2D lamellae of primary ovine VECs by seeding the cells on micropatterned (28) deformable elastomeric substrates. To produce isotropic lamellae, we seeded the endothelial cells on a uniform layer of fibronectin (Fig. 1*A*). When seeded, the cells spread

Author contributions: K.B., J.B., E.A., R.A.L., and K.K.P. designed research; K.B. performed research; K.B., P.W.A., J.W.-S., J.A.G., and A.G. contributed new reagents/analytic tools; K.B. analyzed data; and K.B., P.W.A., J.B., E.A., R.A.L., and K.K.P. wrote the paper.

The authors declare no conflict of interest.

This article is a PNAS Direct Submission.

[1]To whom correspondence should be addressed. E-mail: kkparker@seas.harvard.edu.

This article contains supporting information online at www.pnas.org/lookup/suppl/doi:10.1073/pnas.1106954108/-/DCSupplemental.

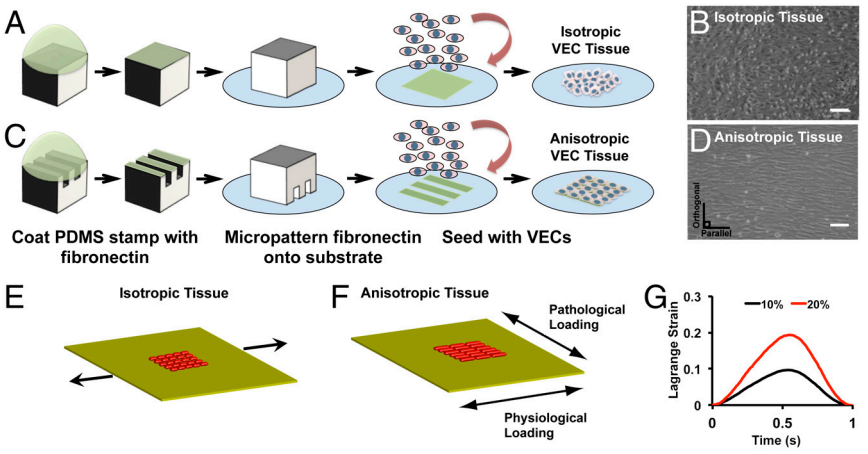

Fig. 1. In vitro experimental model. Isotropic (*A* and *B*) and anisotropic (*C* and *D*) valve endothelial lamellae were engineered via micropatterning of fibronectin and seeding VECs, as shown by phase contrast microscopy. (Scale bar: 100 μm.) Tissue lamellae were engineered on an elastomeric membrane and clamped using aluminum brackets. The silicone membrane can be assembled such that strain can be imposed parallel (physiological) or orthogonal (pathological) to tissue alignment (*E*). Tissue was cyclically stretched at 1 Hz (*F*). Plot of one cycle of Lagrange strain that was representative of low (10%) or high (20%) cyclic strain magnitude (*G*). Schematic of all experimental conditions are shown in Fig S1.

pleomorphically and formed cell–cell junctions with random alignment (Fig. 1*B* and Fig. S1). To build an anisotropic monolayer, we seeded the endothelial cells on alternating lanes of variable fibronectin density (5 and 50 μg/mL) (Fig. 1*C*) where the cells settled and self-organized into an aligned monolayer (Fig. 1*D* and Fig. S1).

These engineered endothelium were assembled into a custom-built, cyclic stretcher device in which the percent strain and direction of stretch relative to tissue architecture could be varied. In our case, in addition to tissue architecture, there were three strain conditions: control (unstretched), 10% (low) (Movie S1), or 20% (high) (Movie S2) cyclic tensile strain at 1 Hz, either parallel or orthogonal to the axis of cell alignment, simulating healthy or diseased conditions, respectively (12, 13) (Fig. 1 *E*–*G* and Fig. S1*B*). In isotropic VEC tissues, actin fibers were randomly arrayed throughout the cell bodies (Fig. 2*A*, *i*), whereas in anisotropic tissues, the actin cytoskeleton aligned with the long axis of the cells, parallel to the underlying fibronectin pattern (Fig. 2*A*, *ii*), as indicated by phalloidin staining. When tissues were cyclically strained (10%) for 24 h, originally VECs in isotropic tissues remodeled with respect to the direction of the applied strain, with elongated cells and alignment of the actin cytoskeleton relative to the direction of stretch (Fig. 2*A*, *iii*). When anisotropic endothelium was stretched parallel to the longitudinal axis of the tissues, increased intercellular alignment of actin fibers was observed (Fig. 2*A*, *iv*), Conversely, when cyclic stretch was applied orthogonal to the longitudinal axis of the anisotropic tissues, actin fiber alignment was disrupted, with alternating regions of actin fibers aligned with stretch, or the underlying fibronectin (Fig. 2*A*, *v*). When the engineered tissues were cyclically stretched for the same time period, but at 20% strain, actin fibers in the isotropic tissues again aligned with the direction of stretch (Fig. 2*A*, *vi*). In anisotropic tissues, stretch parallel to the tissue orientation maintained actin alignment (Fig. 2*A*, *vii*), but when anisotropic tissue was stretched orthogonally, severe disruption of actin fibers was observed relative to those stretched at 10% (Fig. 2*A*, *viii*). We quantified the actin alignment (Fig. S2*A*) with an analysis technique adapted from crystallography (29) to quantify the probability that actin fibers would be coaligned, termed the orientational order parameter (OOP) (30). The actin OOP was significantly greater in anisotropic engineered endothelium stretched 10% parallel to the longitudinal direction versus the actin OOP in the other conditions (Fig. 2*B*). Nuclear morphology reflected local actin alignment, rounder in isotropic tissues, and elongated in anisotropic tissues with the long axis of the nucleus parallel to the cell shape and alignment. Nuclear eccentricity, which is a normalized measure of nuclear elongation (Fig. 2*C*), and cell aspect ratio (Fig. S2 *B* and *C*) largely mimicked actin orientation. Interestingly, the observed alignment of VECs in our tissues with the axis of applied cyclic strain differs from the behavior of vascular endothelial cells (31, 32) but is similar to that of cardiomyocytes (33, 34). These results suggest the ability of cyclic strain to significantly promote or disrupt overall tissue architecture and cell remodeling depending on its magnitude and direction with respect to the initial orientation of the engineered valve endothelium.

Cyclic Strain-Induced EMT of VEC Tissue. The cyclic mechanical loading of the valves during the cardiac cycle has been shown to trig-

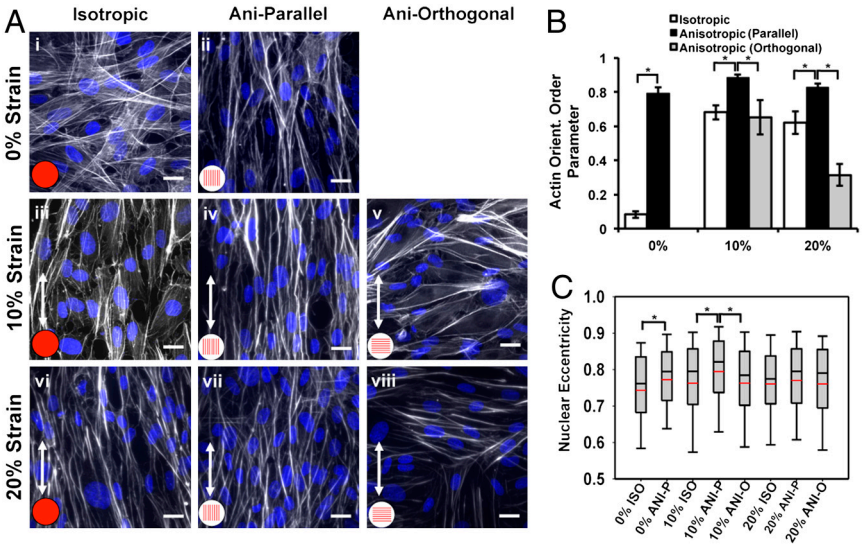

Fig. 2. Cyclic strain resulted in robust tissue alignment and increased actin OOP and nuclear eccentricity. Representative micrographs of actin and DAPI immunostained valve tissue (*A*). (Scale bar: 20 μm.) Actin orientation order parameter (*B*), and nuclear eccentricity (*C*) were quantified for each of the tissue treatments based on the immunostained tissue samples. All graphs, mean ± SEM; $n = 8$; $^*p < 0.05$.

ger a number of cellular processes within the cardiovascular system (17, 35). We asked if cyclic strain potentiated EMT in our engineered valve endothelium via increased expression of the mesenchymal marker α-smooth muscle actin (α-SMA) and downregulation of endothelial markers VE-cadherin and CD31 (36). Isotropic samples cultured at 0% strain (Fig. 3*A*, *i*) were immunonegative for α-SMA expression, indicating that this condition is representative of the static cell culture of VECs. The anisotropic tissues showed some indication of EMT with isolated cells occasionally stained positive for α-SMA within the tissue (Fig. 3*A*, *ii*). In cyclically strained samples, we observed robust increases in α-SMA expression (Fig. 3*A*, *iii*–*viii*). Expression of α-SMA was statistically greater in samples strained to 10% and 20% compared to 0% strain (Fig. 3*B*). At 10% strain, we observed significantly increased α-SMA expression in anisotropic (parallel and orthogonal) samples compared to isotropic samples, whereas at 20% strain, α-SMA expression was maximum in anisotropic-orthogonal tissues, implying a strong link between cell architecture, imposed mechanical strain, and cell phenotype. Western blotting showed that CD31 expression (Fig. 3*C*) was reduced in tissues that underwent EMT, suggesting loss of endothelial phenotype. Quantitative flow cytometry revealed a larger fraction of cells undergoing EMT when cyclic strain was imposed orthogonal to initial tissue alignment (Fig. 3*D*). Our results suggest increased EMT potentiated by cyclic strain. Additionally, the presence of α-SMA-positive stress fibers (Fig. 3*A*) in the transformed cells suggests EMT as a possible adaptive response to mechanical strain with increased contractile myofibroblast expression that is characteristic of VICs (2).

Strain-Induced EMT Results in Altered Tissue Contractile Function. In native valves, VICs can exist as contractile myofibroblasts (37, 38) that respond to vasoactive mediators such as endothelin-1 (ET-1) and serotonin (4, 5). We asked if we could measure the extent of EMT via a functional transformation of the normally noncontractile VEC to a contractile VIC. We modified a muscle tissue contractility assay developed in our laboratory (39, 40) to measure the contractility of transformed cardiac vale tissue, termed a cardiac valve thin film. The vTFs are biohybrid constructs where an engineered tissue adheres to ECM on a polydimethylsiloxane (PDMS) thin film. The vTF bends during cellular contraction and the radius of curvature is an indication of the contractile strength of the tissue (Fig. 4*A*). We examined the response of the cyclically strained anisotropic valve tissues (10% and 20%) to ET-1, potassium chloride (KCl), and the rho-kinase inhibitor HA-1077 versus unstretched controls (Fig. 4*B* and Movie S3). High-strain tissues (20%) generated significantly higher contractile stress in response to ET-1 compared to low-strain tissues (10%) and controls (Fig. 4 *C* and *D*), suggesting transformation of a greater fraction of VECs to the more contractile myofibroblast phenotype under high-strain magnitude. We calculated tissue basal tone by stimulating tissue with an excess of HA-1077 (100 μM). Basal tone of low-strain tissue was significantly higher than control, but significantly lower than high-strain tissue (Fig. 4*E*). Our data suggest that tissues after EMT are likely comprised of transformed, contractile myofibroblast-like cells as shown by greater contractile response and increased basal tone, also supported by strong α-SMA expression reported in the previous section. The fact

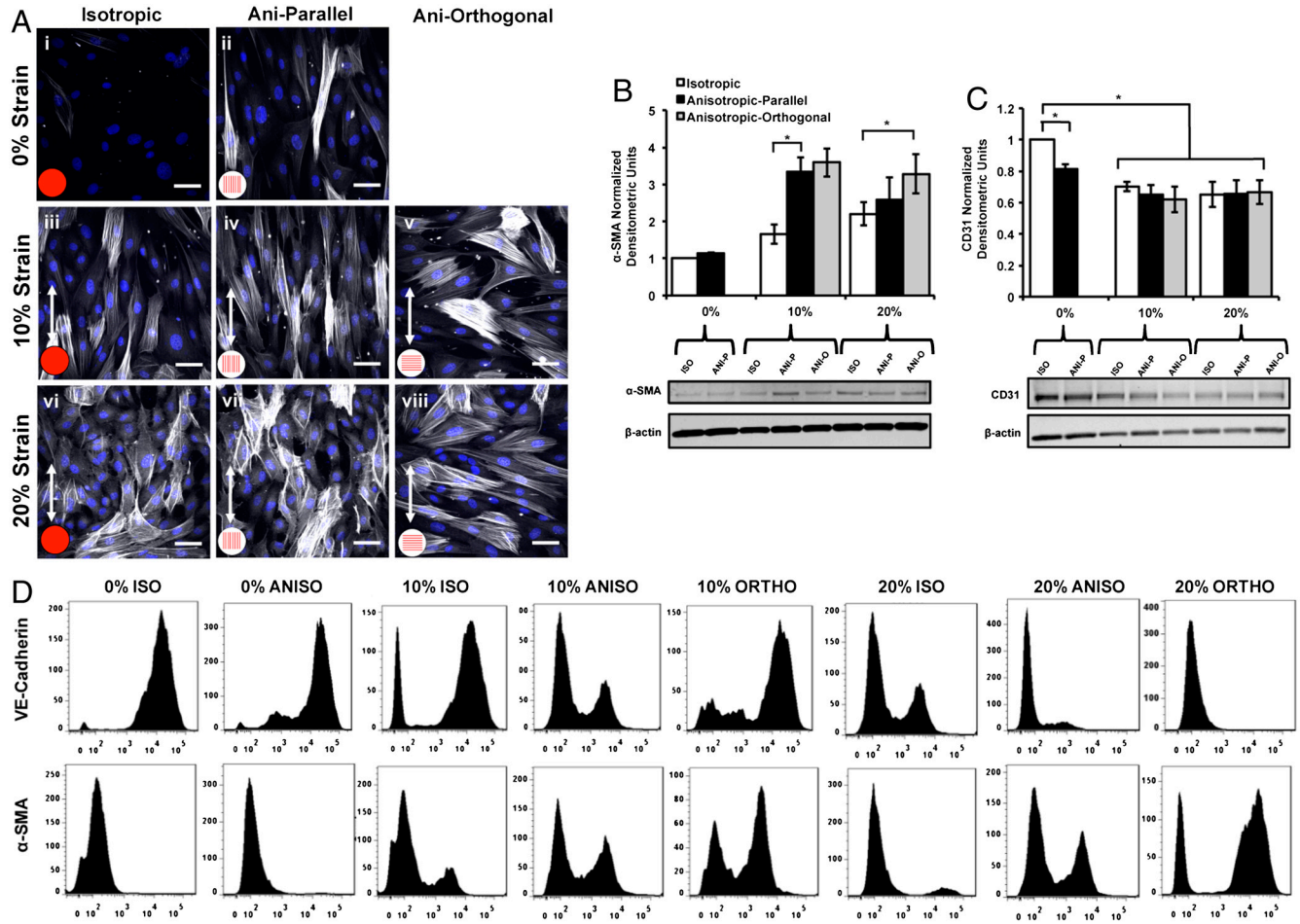

Fig. 3. Cyclic strain resulted in EMT of valve endothelial tissue. Representative micrographs (*A*) VEC tissue stained for DAPI and α-SMA with α-SMA expression indicative of EMT (blue, nuclei; white, α-SMA). (Scale bar: 50 μm.) Western blotting quantitatively demonstrate EMT via increased α-SMA expression (*B*) and reduced CD31 expression (*C*) in samples that were cyclically strained. Quantitative flow cytometry (*D*) also demonstrated EMT via reduced VE-cadherin-positive cells and increased α-SMA-positive cells. All bar graphs, mean ± SEM; $n = 6$; $^*p < 0.05$.

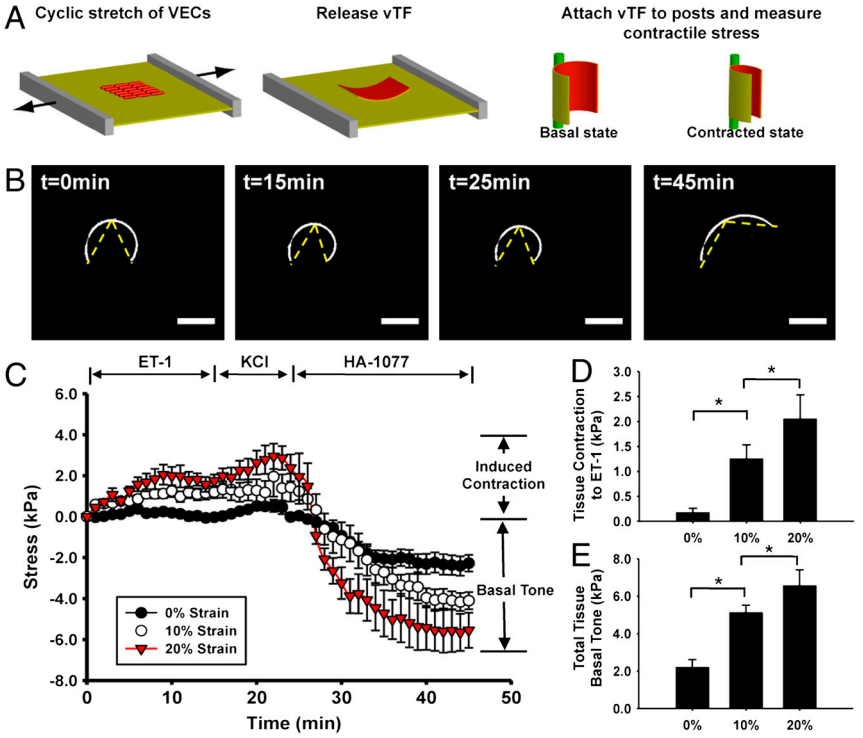

Fig. 4. Valve thin film experiments demonstrating altered tissue function due to cyclic strain-induced EMT. Schematic representation of experimental model (*A*). Anisotropic VEC issue was engineered on an elastic membrane and stretched to induce EMT. Tissue was released from membrane and attached to polytetrafluoroethylene posts to quantify contractile stress response, based on alteration in radius of curvature of tissue samples. Representative thresholded vTF images of 20% strain samples showing initial configuration, contraction after ET-1, KCl, and final relaxed configuration after HA-1077 (*B*). (Scale bar: 1 mm.) Temporal change in tissue stress demonstrated that induced contraction due to ET-1 and KCl, and tissue relaxation following HA-1077 was dependent on strain magnitude (*C*). Induced contractile stress due to ET-1 relative to initial tone in tissues stretched to 0%, 10%, and 20% strain demonstrated strain magnitude-dependent responses (*D*). Total tissue basal tone relative to initial tone in samples stretched to 0%, 10%, and 20% strain demonstrated strain magnitude-dependent responses (*E*). All graphs, mean ± SEM; $n = 8$; $^*p < 0.05$.

that high mechanical strain induced an overall greater contractile phenotype suggests that EMT is an adaptive or injury-response mechanism of the VECs to aberrant cyclic mechanical loading.

Strain-Induced EMT Occurs via Different Pathways Depending on Strain Magnitude. We asked what signaling pathways were activated to induce EMT during cyclic loading, and if there was evidence of an adaptive response depending on strain magnitude. Previous reports suggest that EMT during valve morphogenesis is characterized by reduction in VEGF signaling and elevated TGF-β and wnt/β-catenin signaling (8, 41). We observed reduction in VEGF mRNA in all tissues that underwent EMT (Fig. 5*A*), consistent with these previous studies. TGF-β1 mRNA (Fig. 5*B*) and protein (Fig. 5*C*) expression was significantly increased at 10% strain compared to 0% or 20% strain. We noted phosphorylated-smad-2 (p-smad-2) nuclear expression in 10% strained cells that had undergone EMT (positive α-SMA expression) (Fig. S3*A*), indicating potential activation of the TGF-β signaling pathway. Treatment of tissues with activin receptor-like kinase-4/5/7/smad-2 inhibitor, SB-431542 (42), inhibited smad-2 phosphorylation at both 10% and 20% strain (Fig. S3*C*) but inhibited EMT only at 10% strain (Fig. 5*D*). This result suggests EMT potentiated by TGF-β1/smad-2 signaling at 10% strain and a different mechanism at 20% strain. Immunostaining (Fig. 5*E*) confirmed the expression of β-catenin localized to cell–cell boundaries in all tissues, and also revealed cytosolic expression of β-catenin in anisotropic 20% strained tissues (Fig. 5*E*, *vi* and *vii*). Western blotting (Fig. 5*F*) revealed significantly increased expression of β-catenin in anisotropic 20% strained tissues (parallel and orthogonal), whereas RT-PCR demonstrated increased wnt-1 mRNA expression (Fig. 5*G*) in these same tissues, suggesting EMT occurring via elevated wnt/β-catenin signaling under high (20%) strain. Overall, our results suggest that VECs undergo EMT under both low- and high-strain conditions via different signaling pathways. The former may reflect processes for normal homeostatic renewal of VICs, whereas the latter may indicate an adaptive injury response potentiated by aberrant cyclic mechanical loading.

Discussion

Prior work has focused on the role of soluble mitogens in regulating cardiac valve EMT during development (8, 41, 43–45). Here, we used engineered valve endothelium, with enforced structural characteristics mimicking different regions of the valve, to shed light on a unique role for cyclic strain and tissue architecture in potentiating valve EMT in the adult valve. The indication of increased wnt/β-catenin signaling in the high-stressed VEC structures points to potential reorganization of cell–cell contacts due to orthogonal strain. Additionally, elevated and orthogonally applied cyclic strain on anisotropic tissues caused increased EMT with expression of the myofibroblast phenotype, potentiating increased Rho-associated protein kinase-mediated contractility and basal tissue tone. The strong correlation between strain magnitude and tissue contractility leads us to speculate EMT to be an active, adaptive cellular response. The presence of these contractile cells might also elicit functional changes, leading to a stiffer valve (4), resulting in altered fluid flow patterns and further impaired valve and cardiac function (1, 46). Thus, our results suggest that cardiac valve disease (47) is characterized by abnormal strains leading to cellular reorganization, remodeling (17, 18), EMT, and altered tissue tone and stiffness (48), with activation of signaling pathways observed during valve development.

Cardiac valve EMT shares several common themes with epithelial-mesenchymal transdifferentiation (EpiMT), with both processes manifesting during development (8, 41, 49). Researchers have previously identified a role for cell shape in EpiMT (50) and have identified regions of endogenous mechanical stresses as focal points for EpiMT within tissues (51), with expression of myofibroblast phenotype (52), similar to our observations in this study. Recent work has suggested roles for EpiMT in a variety of pathologies such as cancer metastasis (49) and renal fibrosis (53), and our work suggests potential targets in the form of mechanical strains or molecules such as TGF-β, wnt, and β-catenin for further study.

Finally, our finding of dual-mode potentiation of EMT suggests a more fundamental question: Can we consider EMT as a "waypoint" in the valvular genotypic and phenotypic hyperspace, in order to reach a stable attractor state (balanced population of VECs, and VICs with mesenchymal phenotype) (54, 55)?

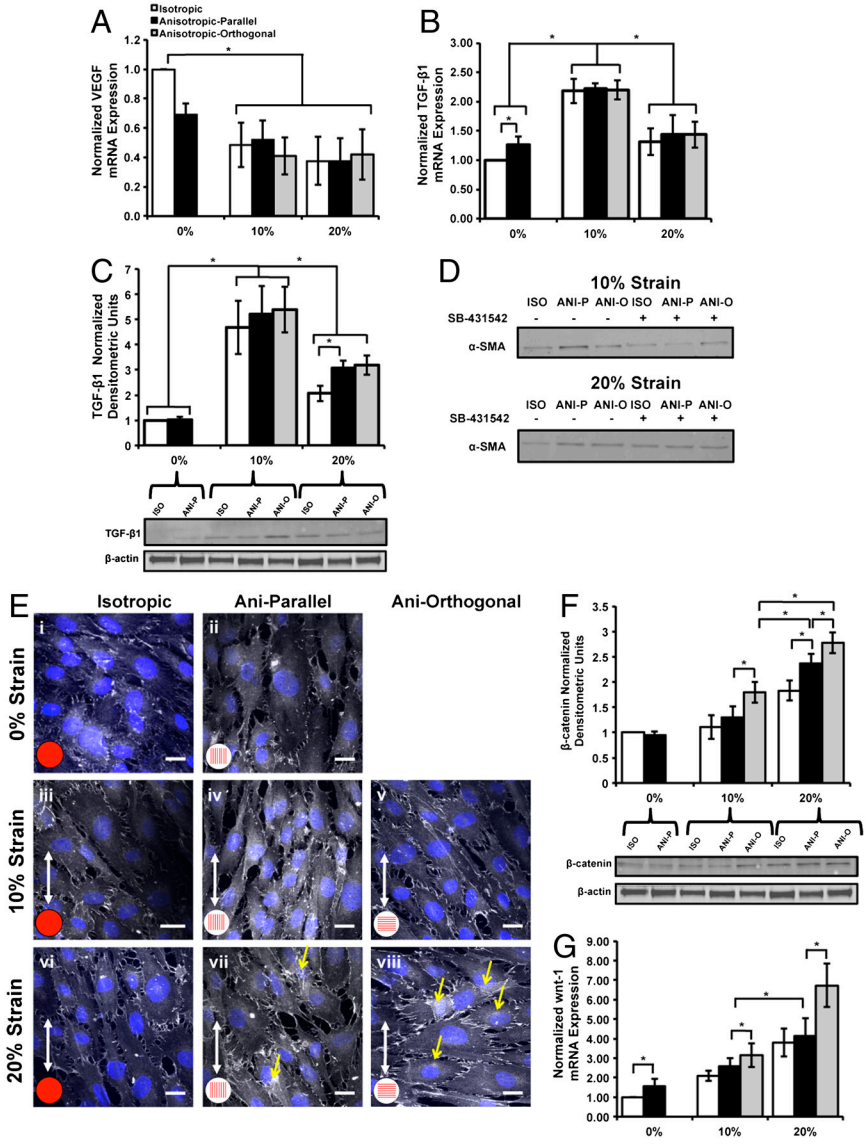

Fig. 5. Dual-mode EMT depending on cyclic strain magnitude. RT-PCR revealed significantly lower VEGF expression in groups that underwent EMT (*A*). TGF-β1 mRNA (*B*) and protein (*C*) expression was significantly higher at low strain (10%) compared to unstretched and high-strain (20%) tissues ($n = 4$). Culture with TGF-β1 antagonist SB-431542 inhibited EMT at 10% strain but not at 20% strain (*D*). Representative micrographs demonstrating normal β-catenin expression (*E*) in 0% and 10% tissue but increased β-catenin staining within cellular cytoplasm (yellow arrows) in tissue stretched orthogonally to high- strain (blue, nuclei; white: β-catenin). (Scale bar: 20 μm.) Western blotting (*F*) demonstrates significantly increased β-catenin expression for tissue stretched to 20% strain compared to 0% or 10% strain. The β-catenin expression was also significantly increased in tissue stretched orthogonal to axis of alignment ($n = 6$). There was significantly increased wnt (*G*) expression at 20% strain and when strain was applied orthogonally to axis of tissue alignment ($n = 4$). All graphs, mean ± SEM; $*p < 0.05$.

Why do we observe EMT in low strain in our model even though that is not commonly observed in healthy adult valves (11)? This acute transformation of VECs suggests that newly engineered VEC lamellae are closer in behavior to developing valves that are primed to undergo exuberant EMT even under normal, low-strain conditions (56). It is also possible that the absence of VIC-like cells, as in our initial VEC tissues, may predispose VECs to undergo EMT to achieve a balanced population of both cell types. Our results suggest a role for EMT in the adult valve as a means for maintaining valve cell phenotype.

Methods

A detailed description of the experimental methods and protocols is included in the *SI Text*. Methods are briefly described below.

Tissue Engineered in Vitro Model of VEC Tissue. We engineered isotropic or anisotropic lamellae of valvular endothelium on elastomeric membranes via micropatterning of fibronectin (28) and seeding VECs to achieve a confluent monolayer (Fig. 1 *A–D*). VEC monolayers were subject to 0% (control), 10%, or 20% uniaxial cyclic strain at 1 Hz for 24 or 48 h using a custom-built cyclic stretcher device (Movies S1 and S2). The latter two strain magnitudes are representative of low- or high-strain regimes in mammalian cardiac valves (27, 57). Cyclic strain was either applied parallel (termed "anisotropic") or orthogonal (termed "anisotropic-orthogonal") to initial tissue alignment, simulating healthy or diseased valves (12, 13). The experimental protocol for cyclic strain is depicted schematically in Fig. S1.

Biochemistry. Immunostaining, flow cytometry, Western blotting, and RT-PCR were performed using standard techniques detailed in the *SI Text*. Primers used for RT-PCR are outlined in Table S1.

Metrics for Cell Alignment. Actin OOP, nuclear eccentricity, and cell aspect ratio were based on computational analyses of immunostained images (30, 58). The OOP was developed for the study of organization of liquid crystals (29) and adapted for biological applications (59), and was computed from the pixel-based orientation vectors of the actin images. The parameter ranges from zero in isotropic systems to one in perfectly aligned systems. Nuclear eccentricity is a normalized expression of nuclear shape, with a perfect circle having a value of zero and a line having a value of one. Cell aspect ratio was quantified via image thresholding cell borders and fitting an ellipse to the outlined shape. Details are in the *SI Text*.

Valve Thin Film Contractile Stress Measurement. Valve thin films were assembled based on a modification of cardiomyocyte thin film technology developed in our laboratory (39, 40). Anisotropic VECs were cyclically strained (0%, 10%, 20%) for 24 h in regular media followed with 24 h of serum starvation to induce a contractile phenotype (60). Free-floating vTFs, which were composed of a layer of aligned valve cells (Fig. S4) on a *ca.* 10-μm layer of PDMS, were released from the underlying elastomeric membrane and attached to polytetrafluoroethylene posts (Fig. 4*A*). The cell layer bends the passive PDMS layer when its tone is altered, resulting in modified curvature of the vTF (Fig. 4*B*), and tissue stress was calculated using methods developed in our laboratory (39). Alteration in tissue function due to EMT was studied via valve tissue response to serial stimulation with the endothelium-derived

vasoconstrictor ET-1 (50 nM), KCl (100 mM), and the rho-kinase inhibitor HA-1077 (100 μM). Optimum ET-1 concentration was based on dose curve experiments on VIC monolayers (Fig. S5), whereas an excess KCl concentration was used to potentiate maximum cell depolarization (61) to allow measurement of the peak contractility of the tissue monolayer (Fig. S5). Excess HA-1077 was used to manifest maximum cell relaxation to enable measurement of tissue basal tone (39).

TGF-β1 Inhibition Experiments. A pharmacological inhibitor for the activin receptor-like kinase-4/5/7/smad-2 inhibitor 4-(5-benzo(1,3)dioxol-5-yl-4-pyridin-2-yl-1H-imidazol-2-yl) benzamide (SB-431542), was added to the culture medium at a concentration of 10 μM (42). Effective inhibitory activity was determined via reduction in expression of phosphorylated-smad-2. Subsequent EMT was analyzed via analysis of α-SMA expression by Western blotting.

ACKNOWLEDGMENTS. We acknowledge funding from the Harvard Catalyst Grant (5UL1RR025758), National Institutes of Health (5U01HL100408-02), Harvard Materials Research Science and Engineering Center, and the Wyss Institute for Biologically Inspired Engineering. The authors also acknowledge the Harvard Center for Nanoscale Systems for the use of clean room facilities.

1. Sacks MS, David Merryman W, Schmidt DE (2009) On the biomechanics of heart valve function. *J Biomech* 42:1804–1824.
2. Taylor PM, Batten P, Brand NJ, Thomas PS, Yacoub MH (2003) The cardiac valve interstitial cell. *Int J Biochem Cell Biol* 35:113–118.
3. Liu AC, Gotlieb AI (2008) Transforming growth factor-beta regulates in vitro heart valve repair by activated valve interstitial cells. *Am J Pathol* 173:1275–1285.
4. El-Hamamsy I, et al. (2009) Endothelium-dependent regulation of the mechanical properties of aortic valve cusps. *J Am Coll Cardiol* 53:1448–1455.
5. Chester AH (2005) Endothelin-1 and the aortic valve. *Curr Vasc Pharmacol* 3:353–357.
6. Chester AH, Misfeld M, Sievers HH, Yacoub MH (2001) Influence of 5-hydroxytryptamine on aortic valve competence in vitro. *J Heart Valve Dis* 10:822–825 discussion 825–826.
7. Chester AH, Misfeld M, Yacoub MH (2000) Receptor-mediated contraction of aortic valve leaflets. *J Heart Valve Dis* 9:250–254 discussion 254–255.
8. Combs MD, Yutzey KE (2009) Heart valve development: Regulatory networks in development and disease. *Circ Res* 105:408–421.
9. Person AD, Klewer SE, Runyan RB (2005) Cell biology of cardiac cushion development. *Int Rev Cytol* 243:287–335.
10. Chaput M, et al. (2009) Mitral leaflet adaptation to ventricular remodeling: Prospective changes in a model of ischemic mitral regurgitation. *Circulation* 120(Suppl 11): S99–103.
11. Dal-Bianco JP, et al. (2009) Active adaptation of the tethered mitral valve: Insights into a compensatory mechanism for functional mitral regurgitation. *Circulation* 120:334–342.
12. Nielsen SL, et al. (1999) Chordal force distribution determines systolic mitral leaflet configuration and severity of functional mitral regurgitation. *J Am Coll Cardiol* 33:843–853.
13. Otsuji Y, et al. (1997) Insights from three-dimensional echocardiography into the mechanism of functional mitral regurgitation: direct in vivo demonstration of altered leaflet tethering geometry. *Circulation* 96:1999–2008.
14. Miquerol L, Gertsenstein M, Harpal K, Rossant J, Nagy A (1999) Multiple developmental roles of VEGF suggested by a LacZ-tagged allele. *Dev Biol* 212:307–322.
15. Paranya G, et al. (2001) Aortic valve endothelial cells undergo transforming growth factor-beta-mediated and non-transforming growth factor-beta-mediated transdifferentiation in vitro. *Am J Pathol* 159:1335–1343.
16. Yang JH, Wylie-Sears J, Bischoff J (2008) Opposing actions of Notch1 and VEGF in postnatal cardiac valve endothelial cells. *Biochem Biophys Res Commun* 374:512–516.
17. Balachandran K, Sucosky P, Jo H, Yoganathan AP (2009) Elevated cyclic stretch alters matrix remodeling in aortic valve cusps—implications for degenerative aortic valve disease? *Am J Physiol Heart Circ Physiol* 296:H756–764.
18. Balachandran K, Sucosky P, Jo H, Yoganathan AP (2010) Elevated cyclic stretch induces aortic valve calcification in a bone morphogenic protein-dependent manner. *Am J Pathol* 177:49–57.
19. Hove JR, et al. (2003) Intracardiac fluid forces are an essential epigenetic factor for embryonic cardiogenesis. *Nature* 421:172–177.
20. Santhanakrishnan A, Miller LA (2011) Fluid dynamics of heart development. *Cell Biochem Biophys* 61:1–22.
21. Miller LA (2011) Fluid dynamics of ventricular filling in the embryonic heart. *Cell Biochem Biophys* 61:33–45.
22. Taber LA, Lin IE, Clark EB (1995) Mechanics of cardiac looping. *Dev Dyn* 203:42–50.
23. Deck JD (1986) Endothelial cell orientation on aortic valve leaflets. *Cardiovasc Res* 20:760–767.
24. Butcher JT, Penrod AM, Garcia AJ, Nerem RM (2004) Unique morphology and focal adhesion development of valvular endothelial cells in static and fluid flow environments. *Arterioscler Thromb Vasc Biol* 24:1429–1434.
25. Yap CH, Saikrishnan N, Yoganathan AP (2011) Experimental measurement of dynamic fluid shear stress on the ventricular surface of the aortic valve leaflet. *Biomech Model Mechanobiol*, in press.
26. Yap CH, Saikrishnan N, Tamilselvan G, Yoganathan AP (2011) Experimental measurement of dynamic fluid shear stress on the aortic surface of the aortic valve leaflet. *Biomech Model Mechanobiol*, in press.
27. Yap CH, et al. (2010) Dynamic deformation characteristics of porcine aortic valve leaflet under normal and hypertensive conditions. *Am J Physiol Heart Circ Physiol* 298: H395–405.
28. Chen CS, Mrksich M, Huang S, Whitesides GM, Ingber DE (1997) Geometric control of cell life and death. *Science* 276:1425–1428.
29. Hamley IW (2007) *Introduction to Soft Matter: Synthetic and Biological Self-Assembling Materials* (Wiley, Hoboken, NJ), Rev. Ed,, pp 18–19.
30. Grosberg A, et al. (2011) Self-organization of muscle cell structure and function. *PLoS Comput Biol* 7:e1001088.
31. Matsumoto T, et al. (2007) Mechanical strain regulates endothelial cell patterning in vitro. *Tissue Eng* 13:207–217.
32. Standley PR, Cammarata A, Nolan BP, Purgason CT, Stanley MA (2002) Cyclic stretch induces vascular smooth muscle cell alignment via NO signaling. *Am J Physiol Heart Circ Physiol* 283:H1907–1914.
33. Yamane M, et al. (2007) Rac1 activity is required for cardiac myocyte alignment in response to mechanical stress. *Biochem Biophys Res Commun* 353:1023–1027.
34. Matsuda T, et al. (2005) N-cadherin-mediated cell adhesion determines the plasticity for cell alignment in response to mechanical stretch in cultured cardiomyocytes. *Biochem Biophys Res Commun* 326:228–232.
35. Balachandran K, et al. (2011) Aortic Valve Cyclic Stretch Causes Increased Remodeling Activity and Enhanced Serotonin Receptor. *Ann Thorac Surg*, 92 pp:147–153.
36. Wylie-Sears J, Aikawa E, Levine RA, Yang JH, Bischoff J (2011) Mitral valve endothelial cells with osteogenic differentiation potential. *Arterioscler Thromb Vasc Biol* 31:598–607.
37. Taylor PM, et al. (2006) Interaction of human valve interstitial cells with collagen matrices manufactured using rapid prototyping. *Biomaterials* 27:2733–2737.
38. Liu AC, Joag VR, Gotlieb AI (2007) The emerging role of valve interstitial cell phenotypes in regulating heart valve pathobiology. *Am J Pathol* 171:1407–1418.
39. Alford PW, Feinberg AW, Sheehy SP, Parker KK (2010) Biohybrid thin films for measuring contractility in engineered cardiovascular muscle. *Biomaterials* 31:3613–3621.
40. Feinberg AW, et al. (2007) Muscular thin films for building actuators and powering devices. *Science* 317:1366–1370.
41. Armstrong EJ, Bischoff J (2004) Heart valve development: Endothelial cell signaling and differentiation. *Circ Res* 95:459–470.
42. Ruiz E, Redondo S, Gordillo-Moscoso A, Tejerina T (2007) Pioglitazone induces apoptosis in human vascular smooth muscle cells from diabetic patients involving the transforming growth factor-beta/activin receptor-like kinase-4/5/7/Smad2 signaling pathway. *J Pharmacol Exp Ther* 321:431–438.
43. Wu B, et al. (2011) Nfatc1 coordinates valve endocardial cell lineage development required for heart valve formation. *Circ Res* 109:183–192.
44. Combs MD, Yutzey KE (2009) VEGF and RANKL regulation of NFATc1 in heart valve development. *Circ Res* 105:565–574.
45. Moskowitz IP, et al. (2011) Transcription factor genes Smad4 and Gata4 cooperatively regulate cardiac valve development. *Proc Natl Acad Sci USA* 108:4006–4011.
46. Sacks MS, Yoganathan AP (2007) Heart valve function: A biomechanical perspective. *Philos trans R Soc London* 362:1369–1391.
47. Markwald RR, Norris RA, Moreno-Rodriguez R, Levine RA (2010) Developmental basis of adult cardiovascular diseases: Valvular heart diseases. *Ann NY Acad Sci* 1188:177–183.
48. Norris RA, et al. (2008) Neonatal and adult cardiovascular pathophysiological remodeling and repair: Developmental role of periostin. *Ann NY Acad Sci* 1123:30–40.
49. Gomes LR, Terra LF, Sogayar MC, Labriola L (2011) Epithelial-mesenchymal transition: Implications in cancer progression and metastasis. *Curr Pharm Biotechnol*, in press.
50. Nelson CM, Khauv D, Bissell MJ, Radisky DC (2008) Change in cell shape is required for matrix metalloproteinase-induced epithelial-mesenchymal transition of mammary epithelial cells. *J Cell Biochem* 105:25–33.
51. Gomez EW, Chen QK, Gjorevski N, Nelson CM (2010) Tissue geometry patterns epithelial-mesenchymal transition via intercellular mechanotransduction. *J Cell Biochem* 110:44–51.
52. Radisky DC, Kenny PA, Bissell MJ (2007) Fibrosis and cancer: Do myofibroblasts come also from epithelial cells via EMT? *J Cell Biochem* 101:830–839.
53. Kriz W, Kaissling B, Le Hir M (2011) Epithelial-mesenchymal transition (EMT) in kidney fibrosis: Fact or fantasy? *J Clin Invest* 121:468–474.
54. Huang S, Eichler G, Bar-Yam Y, Ingber DE (2005) Cell fates as high-dimensional attractor states of a complex gene regulatory network. *Phys Rev Lett* 94:128701.
55. Sheehy SP, Huang S, Parker KK (2009) Time-warped comparison of gene expression in adaptive and maladaptive cardiac hypertrophy. *Circ Cardiovasc Genet* 2:116–124.
56. Aikawa E, et al. (2006) Human semilunar cardiac valve remodeling by activated cells from fetus to adult: Implications for postnatal adaptation, pathology, and tissue engineering. *Circulation* 113:1344–1352.
57. Sacks MS, et al. (2002) Surface strains in the anterior leaflet of the functioning mitral valve. *Ann Biomed Eng* 30:1281–1290.
58. Bray MA, et al. (2010) Nuclear morphology and deformation in engineered cardiac myocytes and tissues. *Biomaterials* 31:5143–5150.
59. Volfson D, Cookson S, Hasty J, Tsimring LS (2008) Biomechanical ordering of dense cell populations. *Proc Natl Acad Sci USA* 105:15346–15351.
60. Han M, Wen JK, Zheng B, Cheng Y, Zhang C (2006) Serum deprivation results in redifferentiation of human umbilical vascular smooth muscle cells. *Am J Physiol Cell Physiol* 291:C50–58.
61. Murray TR, Marshall BE, Macarak EJ (1990) Contraction of vascular smooth muscle in cell culture. *J Cell Physiol* 143:26–38.